Crystal structure of plant pectin methylesterase

Kenth Johansson[a], Mustapha El-Ahmad[a,b], Rosmarie Friemann[a], Hans Jörnvall[b], Oskar Markovič[c], Hans Eklund[a,*]

[a] *Department of Molecular Biology, Swedish University of Agricultural Sciences, S-751 24 Uppsala, Sweden*
[b] *Department of Medical Biochemistry and Biophysics, Karolinska Institutet, S-171 77 Stockholm, Sweden*
[c] *Institute of Chemistry, Slovak Academy of Sciences, 842 38 Bratislava, Slovak Republic*

Received 9 November 2001; revised 17 December 2001; accepted 22 January 2002

First published online 12 February 2002

Edited by Irmgard Sinning

Abstract Pectin is a principal component in the primary cell wall of plants. During cell development, pectin is modified by pectin methylesterases to give different properties to the cell wall. This report describes the first crystal structure of a plant pectin methylesterase. The β-helical structure embodies a central cleft, lined by several aromatic residues, that has been deduced to be suitable for pectin binding. The active site is found at the center of this cleft where Asp157 is suggested to act as the nucleophile, Asp136 as an acid/base and Gln113/Gln135 to form an anion hole to stabilize the transition state.

Key words: Crystal structure; β-Helix; Pectin methylesterase; Plant enzyme; Catalytic mechanism; Binding cleft

1. Introduction

Pectin is a structural carbohydrate found in higher plants. It is located in the primary cell wall and constitutes the principal component of the middle lamella [1]. Pectins are complex molecules that contain a backbone of α(1→4)-linked galacturonic acid chains to which chains of rhamnose and galacturonic acid are bound. Pectins have homogalacturonan-smooth and rhamnogalacturonan-hairy regions [2]. In native pectin, the galacturonic acid units are to a large extent esterified with methanol, thereby forming methyl-D-galactopyranosyl residues. Pectin can be enzymatically deesterified, creating a blockwise distribution of deesterified homogalacturonan units [3]. This reaction takes place during plant growth where highly methyl-esterified homogalacturonan deposited in cell walls is deesterified [4]. Deesterified blocks can be cross-linked with calcium, resulting in gel formation which contributes to intercellular adhesion. The pattern of methyl esters is likely to contribute distinct mechanical and porosity properties to the cell wall matrix.

Methyl-D-galactopyranosyl residues of pectin are substrates for pectin methylesterase (PME) (EC 3.1.1.11). PMEs catalyze the pectin deesterification by forming carboxylates and methanol. The plant PMEs possess a role in cell wall metabolism by preparing the substrate for the action of polygalacturonases and pectate lyases. The abundance of pectin-degrading enzymes at different growth stages in plants suggests that these enzymes play important roles in development, dormancy breakage, seed and pollen germination, fruit ripening, etc. [5–7]. PMEs also act in defense mechanisms of plants against pathogens [8]. PME is present in all higher plants and is particularly abundant in citrus fruits and vegetables. PMEs are also produced by pathogenic bacteria and fungi. Pectins, particularly from orange peel and apple pomace, are used industrially [9]. While gelation of high-methoxy pectin is dependent on the presence of significant quantities of sugar, low-methoxy pectin may be induced to gel by the addition of metal ions in the absence of sugar. Use of the latter pectin substrate makes it possible to manufacture jams and jellies of low sugar content.

Plant PMEs typically occur as multigene isoenzymes [10–12], and it is generally proposed that they remove methyl esters in a processive, blockwise fashion (single chain mechanism), giving rise to domains of contiguous, deesterified galacturonic acid residues [3]. In contrast, the action of fungal PMEs (*Aspergillus* sp.) is regarded as random (or multiple chain mechanism) [13–15]. However, the fungal PME from *Trichoderma reesei* deesterifies pectin in blocks [16], and pectin deesterification in *Erwinia chrysanthemi* PME is similar to that of plant PMEs [17]. It therefore appears that the mode of deesterification by PMEs is independent of the origin (microbial or plant) but is rather determined by enzyme properties characterized by p*I* and pH optimum [16].

The only known three-dimensional structure of a PME so far is for a bacterial enzyme produced by *E. chrysanthemi*, PemA (P07863) [18]. This structure has a right-handed parallel β-helix as seen in all bacterial and fungal pectic enzymes: in pectate lyases [19–21], pectin lyases [22,23], polygalacturonases [24,25] and rhamnogalacturonase [26]. The structure of the bacterial PME from *E. chrysanthemi* showed convincingly that PME is a new type of hydrolase which contains neither an α/β hydrolase fold nor a catalytic Ser-His-Asp triad [18]. Instead, PMEs appear to be carboxylate hydrolases with two aspartic acid residues at the active site. This was not surprising since previous studies had already excluded that tomato PME could be a serine esterase [27] and had also shown that there is no conserved histidine or serine residue as a potential catalytic residue in the PME primary structures [18]. Furthermore, modification of histidine residues in tomato and *Aspergillus niger* PMEs demonstrated that these residues do not have active site function, but contribute to overall structural stability [28].

We have now determined the first three-dimensional struc-

*Corresponding author. Fax: (46)-18-53 69 71.
E-mail address: hasse@xray.bmc.uu.se (H. Eklund).

PII: S0014-5793(02)02372-4

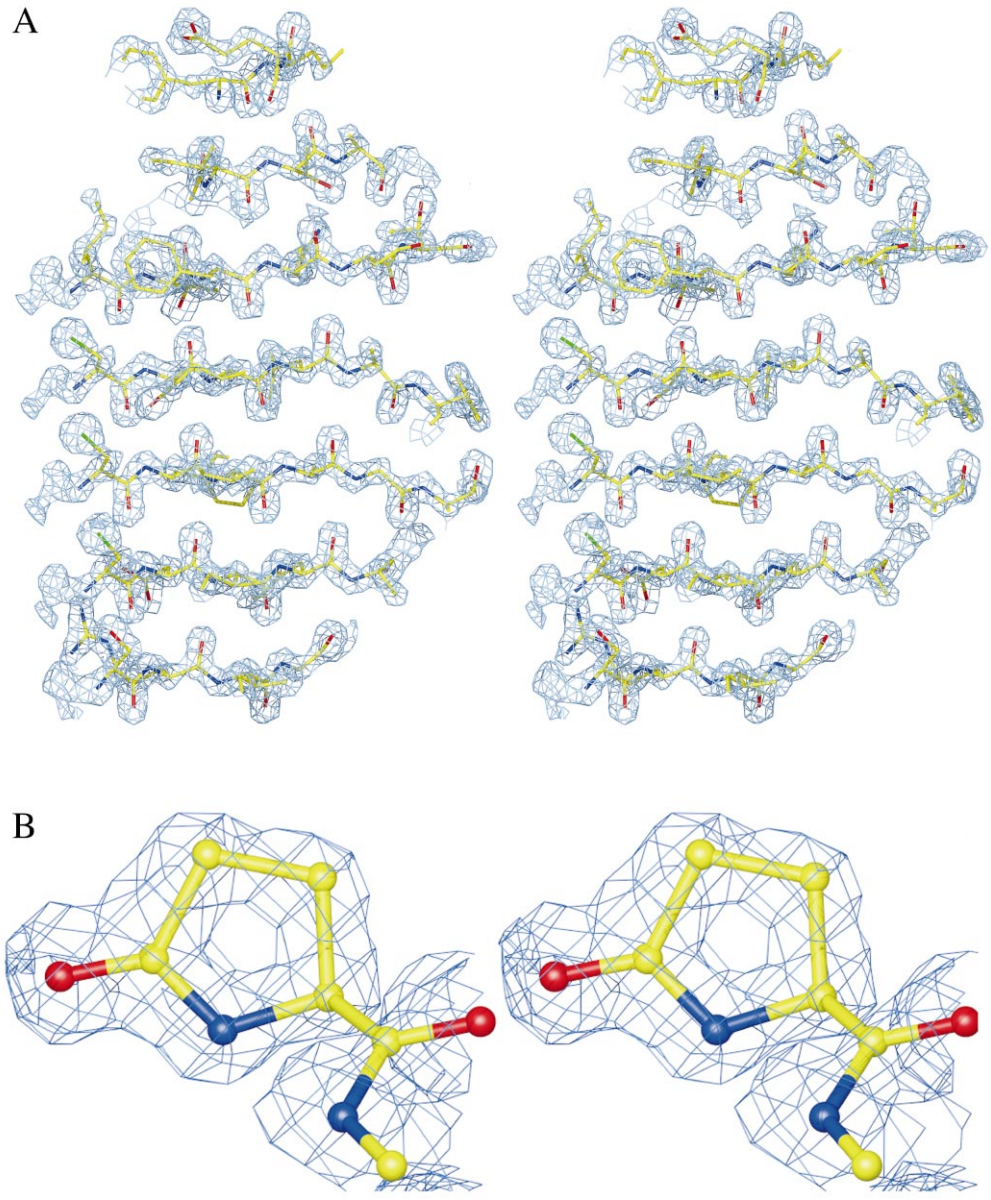

Fig. 1. Stereo figures of the electron density maps at 1.75 Å resolution. A: Electron density map of the PB2 sheet ($2F_o-F_c$) contoured at 1σ after ARP/wARP modeling and initial refinement. Notice the stacking of three internal cysteines at the left of the figure. B: In the final electron density map ($2F_o-F_c$ contoured at 1σ), the cyclic N-terminal pyroglutamate residue was visible. Figures were made by O-plot [35].

Table 1

Space group	$P2_12_12$
Resolution range (last shell)	25–1.75 (1.80–1.75)
Unit cell	$a=49.49$ Å, $b=77.63$ Å, $c=89.22$ Å
Unique reflections	35 380
Redundancy (last shell)	3.5 (3.4)
R_{sym} (last shell) (%)	7.3 (29.1)
Completeness (last shell) (%)	99.6 (98.6)
$I/\sigma(I)$ (last shell)	9.6 (2.6)
R-factor/R_{free} (%)	18.2/19.3
RMS deviation from ideality	
Bonds (Å)	0.008
Angles (°)	1.5
Average B-factors (Å^2)	
Protein	8.4
Solvent	22.3
Cacodylate	11.6
Wilson plot B-factor	10

ture of a plant PME. The structure was determined by molecular replacement methods using the bacterial enzyme from *E. chrysanthemi* as the search model. The structure, refined at 1.75 Å resolution, shows a long cleft along the molecule suitable for pectin binding. An enzymatic mechanism based on conserved residues in the center of the cleft is suggested.

2. Materials and methods

2.1. Purification and crystallization of carrot PME

PME was prepared from ripe carrot roots (*Daucus carota*) by homogenization and extraction with 2 M NaCl at pH 7.8, as previously described [29]. The extract was precipitated with ammonium sulfate (saturation 30–75%) and purified by ion exchange (DEAE-Sephadex A-50 and CM-Sephadex C-50) and size exclusion chromatography (Sephadex G-75 and FPLC Superose 12). The homogeneity of the isolated PME was proven by SDS–PAGE (one single band with M_r close to 33 000), isoelectric focusing (one band with p$I=9.8$) and

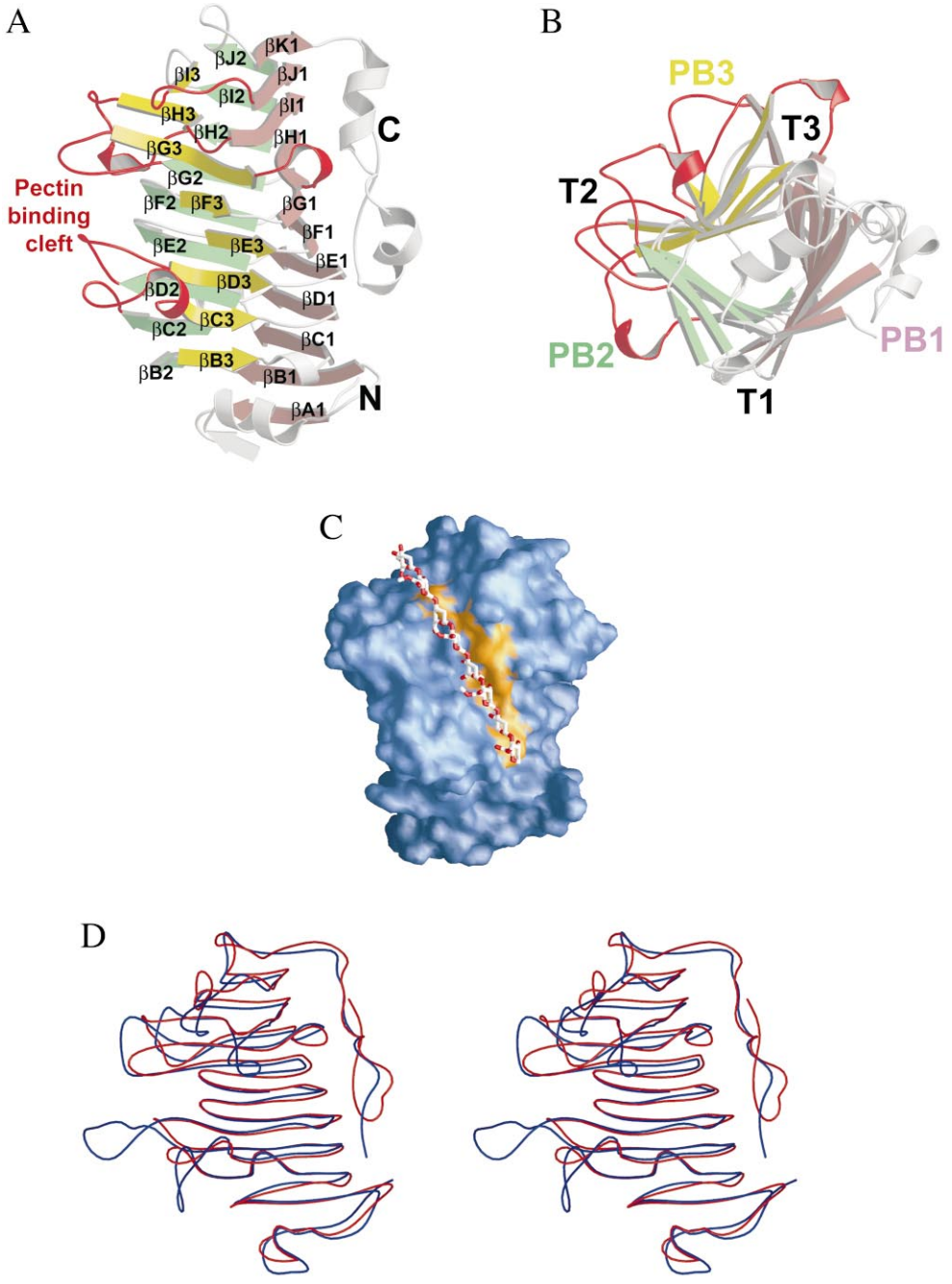

Fig. 2. The structure of carrot PME. A: The carrot PME has a β-helix structure consisting of three parallel β-sheets organized in a prism-like fashion. The sheets PB1, PB2 and PB3 are colored brown, green and yellow, respectively. Strands are numbered from βA1 to βK1 in sheet PB1, βB2 to βJ2 for sheet PB2 and βB3 to βI3 for sheet PB3. Loops forming the pectin binding cleft are in red; parts not participating in the β-sheets are in white. B: View of the structure rotated 90° around the *x*-axis, looking down from the N-terminal side. Coloring is the same as above. The location of PB1, PB2 and PB3 as well as loops between the sheets, called T1, T2 and T3, are indicated. The figures were made using Molscript [39]. C: Surface representation of the pectin binding cleft. Loops from T2 and T3 form the walls of a cleft running across the molecule. Aromatic residues (in orange) are lining the cleft, as seen in other carbohydrate binding proteins. A pectin molecule is modeled in approximately 2_1-helix conformation. The figure was made using GRASP [40]. D: Superposition of the two known structures of PMEs. Stereo view of the carrot PME (red) superimposed on the *E. chrysanthemi* PME structure (blue). The view is the same as in A. The structures are very similar and 268 Cα atoms can be superimposed with an rmsd of 1.3 Å. The largest differences are located in the loop regions where the *E. chrysanthemi* enzyme has distinctly longer loops, making the walls of the substrate cleft markedly higher.

determination of C-terminal amino acid (Leu); the N-terminus is pGlu, which is resistant to Edman degradation. The enzyme concentration was determined using A_{280} with the extinction coefficient 23.4 at 1% and 1 cm. The specific activity of carrot PME used for crystallization was 32 mol/s/kg, and the K_m value was 1.5×10^{-6}.

Crystallization conditions were tested using Crystal screen I and II (Hampton research) and subsequently optimized. Crystals were grown using the hanging drop vapor diffusion method. The crystallization solution, consisting of 0.2 M sodium acetate, 0.1 M sodium cacodylate, pH 6.5, and 30% PEG 8000, was mixed with an equal volume of a protein solution at a concentration of 10 mg/ml. Typically, the crystals grow to a size of $60\times50\times25$ μm^3 in 3–4 weeks at 14°C.

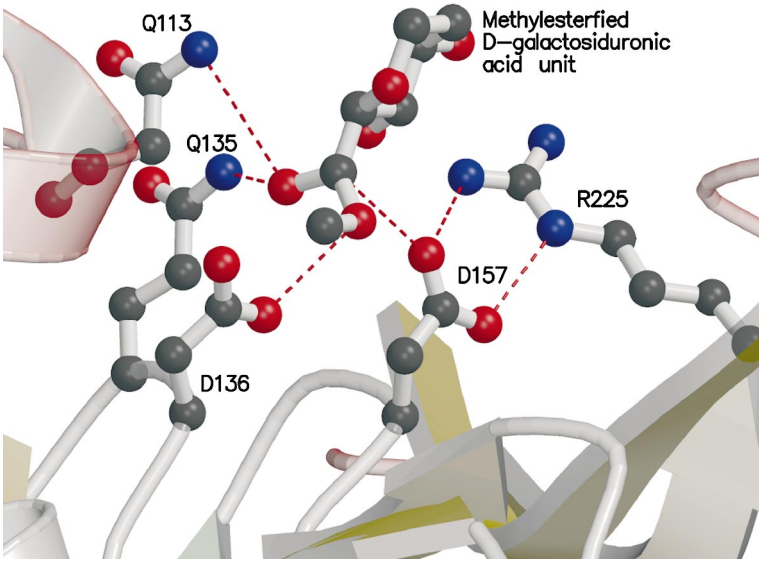

Fig. 3. The active site. The substrate, a methylesterified D-galactosiduronic acid unit, is modeled in the active site. Arg225 is hydrogen-bonded to Asp157, which is suitably positioned for nucleophilic attack on the carboxymethyl carbon, while Asp136 would act as an acid/base during catalysis. The two glutamine residues, Gln113 and Gln135, could form an anion hole for stabilization of the negatively charged tetrahedral intermediate.

2.2. Data collection

Data collection was performed on beamline 711 at MaxII in Lund, Sweden, using a MAR345 image plate. Data were collected at 100 K on a crystal frozen in liquid nitrogen. The cryo solution consisted of the crystallization solution with an addition of 15% PEG 400. The crystals diffract to a limit of 1.75 Å and belong to the primitive orthorhombic space group $P2_12_12$. The data were indexed, scaled and merged using Mosflm [30] and Scala [31,32] (for statistics, see Table 1). The crystals have one molecule in the asymmetric unit, corresponding to a solvent content of 40%.

2.3. Structure determination and refinement

The structure of carrot PME was solved by molecular replacement using the program AMoRe [33]. The coordinates of the *E. chrysanthemi* PME with a sequence identity of 31%, including all side chains (pdb code 1qjv) were used as a search model. Initially, a round of simulated annealing was performed on the full model of 1qjv, using the program CNS [34]. From the resulting $2F_o-F_c$ and F_o-F_c maps, we were able to find about two-thirds of the polypeptide chain using O [35]. This rather poor partial model (R/R_{free} = 40/45%) was then used for initial phasing for the program ARP/wARP [36], which resulted in a map (Fig. 1A) and model of excellent quality (R/R_{free} = 18/23%). 5% of the reflections are used for R_{free} calculations. Further refinement was carried out using the program Refmac5 [31,37] and CNS [34]. The final model accounts for all 319 amino acid residues, 346 water molecules and two cacodylate ions. The coordinates and structure factors have been deposited at the protein data bank (code 1gq8).

3. Results and discussion

3.1. Structure quality

The structure of carrot PME has been refined at 1.75 Å resolution to a *R*-value of 18.2% (R_{free} 19.3%) with good stereochemistry (see Table 1). There are two Ramachandran plot outliers, His112 and Asn143, both with well-defined electron density. His112 is close to the active site, whereas Asn143 is present in a sharp bend between sheets. All residues in the molecule were located in the electron density map. The three N-terminal residues had weak density indicating higher flexibility. However, the unusual cyclic N-terminal pGlu [41] was visible as a circular density (Fig. 1B). Only a handful of side chains, mainly from lysine residues at the surface, have undefined density. Four residues, Gln104, Asn149, Arg176 and Lys309, were found to have two different side chain conformations.

3.2. Structure of carrot PME

PME belongs to the family of parallel β-helix proteins. The β-prism organization of these has been described as consisting of three parallel β-sheets, PB1, PB2 and PB3 [19], whereas the turns between the strands in PB1–PB2, PB2–PB3 and PB3–PB1 are called T1, T2 and T3, respectively (Fig. 2A,B). The carrot PME has eight regular β-helix turns with strands in all three sheets. Furthermore, PB1 contains one extra parallel strand at the N-terminal side of the sheet and two at the C-terminal side, whereas PB2 has one extra strand at the C-terminal side of the β-helix. We refer to the strands in the sheets as βA1, βB2, etc. where 1–3 refer to the β-sheet and A–K refer to the layer of the β-helix (Fig. 2A). The turns will be referred to as TC3 etc. in an equivalent way.

PB1 is the largest, most regular sheet in the structure. The smoothly curved 11-stranded parallel sheet has the first and last strands roughly perpendicular to each other. Similarly, PB2 is a smoothly curved 10-stranded β-sheet where only the C-terminal strand is distorted at the end with a β-turn. PB3 is systematically distorted by β-bulges in strands βD3–βH3 where residues, 116, 137, 158, 185 and 223 kink the sheet and distort locally the parallel hydrogen-bonding pattern. The N-terminal seven residues before the first β-strand have no secondary structure. Between the first strands of PB1, there is a short antiparallel strand, β1, at the edge of the long β-helix and an α-helix, α1, at the edge of PB3. The last 30 residues at the C-terminus form a series of short disordered helices, and a tail of residues 312–319, without secondary structure on the outside of PB1.

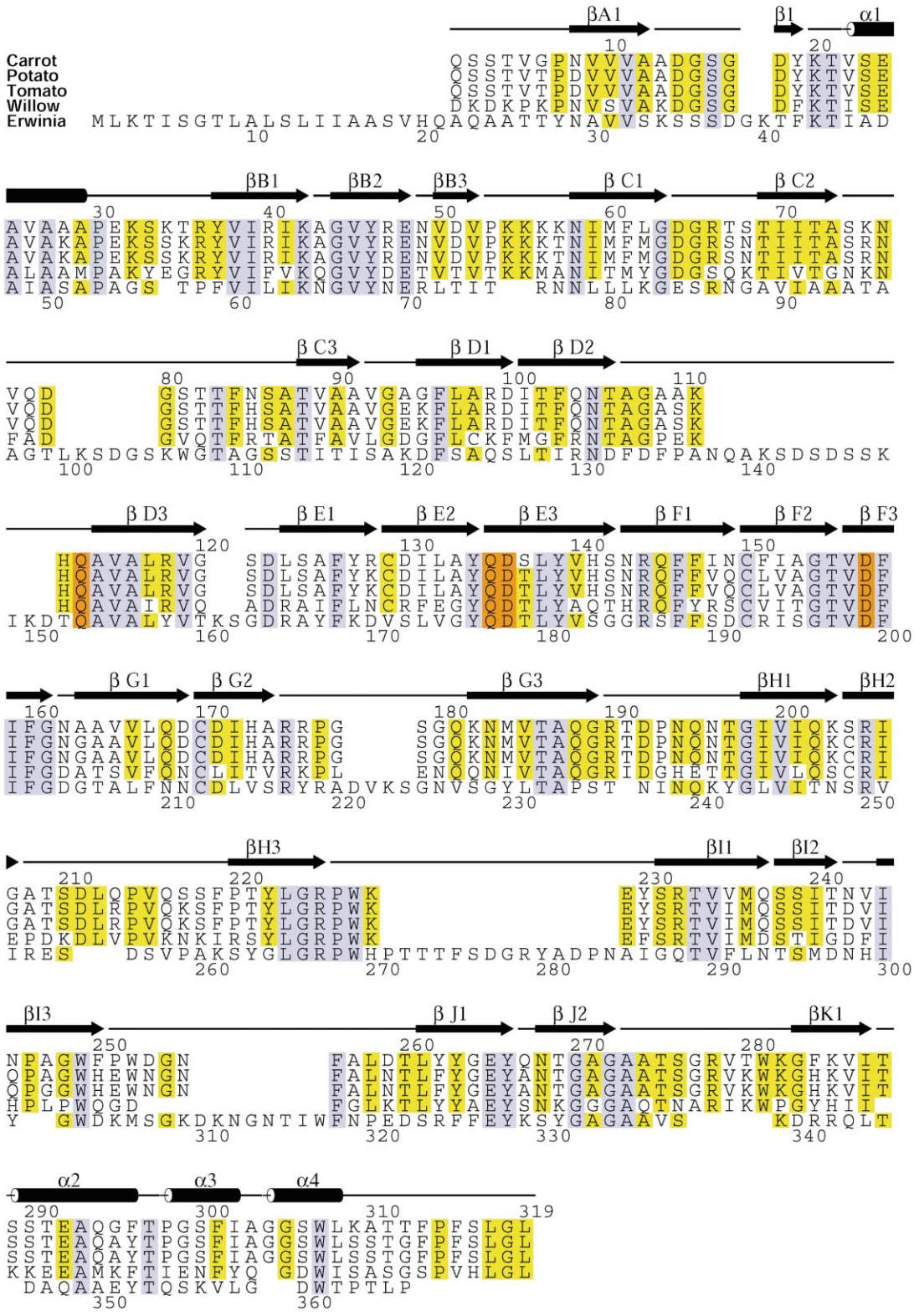

Fig. 4. Structurally based sequence alignment of PMEs. The sequences of five different PMEs are aligned. The top four sequences are from plants and are aligned according to sequence, while the bottom sequence from *E. chrysanthemi* is aligned according to a structural comparison with the carrot PME structure. Residues conserved in all sequences are colored blue while those conserved in four out of five sequences are in yellow. The sequence identities between the carrot PME sequence (SwissProt Accession No. P83218) [41] and the sequences of PMEs from potato (EMBL: AF152172), tomato leaves (GenBank: U49330), willow (EMBL: AB029461) and *E. chrysanthemi* (GenBank: Y00549) are 87%, 85%, 52% and 31%, respectively. The proposed active site residues are all conserved and are indicated in orange. The N-terminal Gln in the carrot enzyme is post-translationally modified to a cyclic pGlu. The figure was made using Alscript [42].

The T1 turn regions are short with generally no residue or only one residue connecting strands in PB1 and PB2. The only exception is TC1 which is five residues long. The T2 and T3 turn regions often contain longer loops. A cleft on one side of the molecule is formed by TC2, TD2, TG2 and TH2 shaping one wall and TG3, TH3 and TI3 the other (Fig. 2A,B).

The space inside the β-helix structure is essentially hydrophobic. There is no asparagine ladder in PME as has been described for pectate lyase [19]. A similar example of an internal stacking ladder is formed by Cys129, Cys150 and Cys170 in three consecutive strands (Fig. 1a). No disulfide bridge exists in the structure. Interestingly, two disulfide bridges have been reported in the homologous tomato fruit PMEs [38]. One of the disulfide bridges in the tomato fruit PME was formed between the residue corresponding to Cys170 and a cysteine corresponding to Ser204 in the carrot enzyme (Fig. 4) in a stacking position on the adjacent strand.

3.3. The pectin binding site

The long shallow cleft across the molecule has all the properties expected for the pectin binding site. The central part of this cleft is lined by several aromatic residues, as is characteristic for carbohydrate binding sites. These include Phe84, Tyr139, Phe160, Tyr222, Trp227, Phe250 and Trp252. Modeling of a pectin molecule in roughly 2_1-helix configuration (with the carboxymethyl groups pointing in different directions in successive carbohydrate residues) can be accommodated in this cleft (Fig. 2C).

3.4. The active site

The active site of carrot PME is located in the long shallow cleft with two carboxylate residues in the center, Asp136 and Asp157. Both these residues are located as the second residue in a PB3 strand and there is about 4.5 Å between the carboxylate groups of these residues. Asp157 is hydrogen-bonded with both side chain oxygens to Arg225. Asp136 has no side chain hydrogen bond to any protein atoms (Fig. 3). There is a non-protein density in the active site which may be a cacodylate ion from the crystallization solution. This ion is bound in the active site in contact with both of the aspartate residues and with two glutamine side chains, Gln113 and Gln135, and two aromatic residues, Phe160 and Trp227.

3.5. Mechanism of action

PMEs hydrolyze the ester bond of methylated galacturonid units, producing a negatively charged polymer and methanol. From the structure, the following mechanism of action can be suggested: Asp157, which is hydrogen-bonded with both side chain oxygens to Arg225, is suggested to be the nucleophile for the primary attack on the carboxymethyl carbonyl carbon. In analogy with other hydrolytic mechanisms, a tetrahedral, negatively charged intermediate could then be stabilized by an anion hole formed by the two glutamine side chains 113 and 135. Asp136, which has a more buried position close to Phe160, may act as an acid in the first cleavage step, where methanol is leaving. Asp136 could then in the next step act as a base, extracting a hydrogen from an incoming water molecule to cleave the covalent bond between the substrate and Asp157 to restore the active site. In an alternative mechanism suggested by Jenkins et al. [18], an active site aspartate is suggested to be responsible for the deprotonation of a catalytic water molecule, in the manner of aspartic proteases, rather than a direct nucleophile attack by an aspartate residue.

It has been shown that both plant and bacterial PMEs perform the catalysis with some processivity, i.e. the enzyme forms blocks of demethylated pectin by catalyzing the hydrolysis of a number of successive methylated galacturonid units along the pectin chain. The catalysis produces a negatively charged carboxylate product which may be repelled from the active site with its two aspartic residues. The interactions between the pectin polymer and the long substrate cleft with its aromatic rings should be sufficient to keep the substrate bound to the enzyme for additional cycles.

3.6. Comparison with the E. chrysanthemi PME

The general structure of the carrot PME and the bacterial enzyme from *E. chrysanthemi* is very similar, and about two-thirds of the residues (268 Cα-atoms) can be superimposed with an rmsd of 1.3 Å (Fig. 2D). The main differences are the much longer loops in the *E. chrysanthemi* enzyme, making the walls of the substrate cleft higher. It is primarily connections TC2, TD2, TH3 and TI3 which are significantly longer in the bacterial enzyme. All these loops have different conformations in the two enzymes.

The structures also differ in the termini. The short antiparallel strand β1 at the N-terminus corresponds to a loop without secondary structure in the *E. chrysanthemi* enzyme. The last turn of the β-helix also differs; where the carrot enzyme has the last strand of PB1 there is just a short strand with two hydrogen bonds in the *E. chrysanthemi* enzyme. The C-terminus in the carrot enzyme contains an additional helix and has a longer extended chain at the end than *E. chrysanthemi* PME.

3.7. Comparison with other plant PMEs

The sequence similarity among the plant PMEs is high (Fig. 4) and residues at the active site are conserved: the two aspartic acids, the arginine, the two glutamines and most of the aromatic residues lining the cleft. Furthermore, there are only minor differences in chain length for a few plant enzymes. Thus, the structure of carrot PME described here can be considered a prototype for the whole family of plant PMEs and can serve as a basis for future structure–function studies.

Acknowledgements: This work was supported by grants from the Swedish Natural Science Research Council and from the Slovak Grant Agency for Science (to O.M.).

References

[1] Roberts, K. (1990) Curr. Opin. Cell Biol. 2, 920–928.
[2] Schols, H.A., Vierhuis, E., Bakx, E.J. and Voragen, A.G. (1995) Carbohydr. Res. 275, 343–360.
[3] Willats, W.G., Orfila, C., Limberg, G., Buchholt, H.C., van Alebeek, G.J., Voragen, A.G., Marcus, S.E., Christensen, T.M., Mikkelsen, J.D., Murray, B.S. and Knox, J.P. (2001) J. Biol. Chem. 276, 19404–19413.
[4] Femenia, A., Garosi, P., Roberts, K., Waldron, K.W., Selvendran, R.R. and Robertson, J.A. (1998) Planta 205, 438–444.
[5] Ren, C. and Kermode, A.R. (2000) Plant Physiol. 124, 231–242.
[6] Micheli, F., Sundberg, B., Goldberg, R. and Richard, L. (2000) Plant Physiol. 124, 191–199.
[7] Pilatzke-Wunderlich, I. and Nessler, C.L. (2001) Plant Mol. Biol. 45, 567–576.
[8] Colmer, A. and Keen, N.T. (1986) Annu. Rev. Phytopathol. 24, 383–409.

[9] Thakur, B.R., Singh, R.K. and Handa, A.K. (1997) Crit. Rev. Food Sci. Nutr. 37, 47–73.
[10] Hall, L.N., Bird, C.R., Picton, S., Tucker, G.A., Seymour, G.B. and Grierson, D. (1994) Plant Mol. Biol. 25, 313–318.
[11] Goldberg, R., Pierron, M., Bordenave, M., Breton, C., Morvan, C. and du Penhoat, C.H. (2001) J. Biol. Chem. 276, 8841–8847.
[12] Sexton, A.C., Paulsen, M., Woestemeyer, J. and Howlett, B.J. (2000) Gene 248, 89–97.
[13] Ishi, S., Kiho, K., Sugiiyama, S. and Sugimoto, H. (1979) J. Food Sci. 44, 611–614.
[14] Kohn, R., Markovič, O. and Machová, E. (1982) Collect. Czech. Chem. Commun. 48, 790–797.
[15] Limberg, G., Korner, R., Buchholt, H.C., Christensen, T.M., Roepstorff, P. and Mikkelsen, J.D. (2000) Carbohydr. Res. 327, 293–307.
[16] Markovič, O. and Kohn, R. (1984) Experientia 40, 842–843.
[17] Christensen, T.M.I.E., Brunstedt, J., Buchholt, H.C. and Mikkelsen, J.D. (2001) in: Pectins and Pectinases 2001. Book of Abstracts of an International Symposium, Rotterdam, The Netherlands, May 6–11, p. 83.
[18] Jenkins, J., Mayans, O., Smith, D., Worboys, K. and Pickersgill, R.W. (2001) J. Mol. Biol. 305, 951–960.
[19] Yoder, M.D., Lietzke, S.E. and Jurnak, F. (1993) Structure 1, 241–251.
[20] Yoder, M.D., Keen, N.T. and Jurnak, F. (1993) Science 260, 1503–1507.
[21] Lietzke, S.E., Scavetta, R.D., Yoder, M.D. and Jurnak, F. (1996) Plant Physiol. 111, 73–92.
[22] Mayans, O., Scott, M., Connerton, I., Gravesen, T., Benen, J., Visser, J., Pickersgill, R. and Jenkins, J. (1997) Structure 5, 677–689.
[23] Vitali, J., Schick, B., Kester, H.C., Visser, J. and Jurnak, F. (1998) Plant Physiol. 116, 69–80.
[24] Pickersgill, R., Smith, D., Worboys, K. and Jenkins, J. (1998) J. Biol. Chem. 273, 24660–24664.
[25] van Santen, Y., Benen, J.A., Schroter, K.H., Kalk, K.H., Armand, S., Visser, J. and Dijkstra, B.W. (1999) J. Biol. Chem. 274, 30474–30480.
[26] Petersen, T.N., Kauppinen, S. and Larsen, S. (1997) Structure 5, 533–544.
[27] Markovič, O. and Patočka, J. (1977) Experientia 33, 711–712.
[28] Markovič, O., Stovíčkova, J. and Jörnvall, H. (1996) J. Protein Chem. 15, 127–130.
[29] Stratilová, E., Markovič, O., Dzúrová, M., Malovíkova, A., Capek, P. and Ornelková, J. (1998) Biologia Bratislava 53, 731–738.
[30] Powell, H.R. (1999) Acta Crystallogr. D55, 1690–1695.
[31] CCP4 (1994) Acta Crystallogr. D50, 760–763
[32] Evans, P.R. (1997) Joint CCP4 ESF-EACBM Newslett. 33, 22–24.
[33] Navaza, J. (1994) Acta Crystallogr. 50, 157–163.
[34] Brünger, A.T., Adams, P.D., Clore, G.M., DeLano, W.L., Gros, P., Grosse-Kunstleve, R.W., Jiang, J.S., Kuszewski, J., Nilges, M., Pannu, N.S., Read, R.J., Rice, L.M., Simonson, T. and Warren, G.L. (1998) Acta Crystallogr. D54, 905–921.
[35] Jones, T.A., Zou, J.Y., Cowan, S.W. and Kjeldgaard, M. (1991) Acta Crystallogr. 47, 110–119.
[36] Perrakis, A., Morris, R. and Lamzin, V.S. (1999) Nature Struct. Biol. 6, 458–463.
[37] Murshudov, G.N., Vagin, A.A. and Dodson, E.J. (1997) Acta Crystallogr. D53, 240–255.
[38] Markovič, O. and Jörnvall, H. (1992) Protein Sci. 1, 1288–1292.
[39] Kraulis, P. (1991) J. Appl. Crystallogr. 24, 946–950.
[40] Nicholls, A., Sharp, K.A. and Honig, B. (1991) Proteins 11, 281–296.
[41] Markovič, O., Cederlund, E., Griffiths, W.J. and Jörnvall, H. (2002) Characterization of carrot pectin methylesterase, Cell Mol. Life Sci. 59, in press.
[42] Barton, G.J. (1993) Protein Eng. 6, 37–40.